Electro-osmotically induced convection at a permselective membrane

I. Rubinstein* and B. Zaltzman†
Jacob Blaustein Institute for Desert Research, Ben-Gurion University of the Negev, Sede-Boqer Campus, 84990, Israel
(Received 18 January 2000)

The paper is concerned with convection at an ion exchange electrodialysis membrane induced by nonequilibrium electro-osmosis in the course of concentration polarization under the passage of electric current through the membrane. Derivation of nonequilibrium electro-osmotic slip condition is recapitulated along with the linear stability analysis of quiescent electrodiffusion through a flat ion exchange membrane. Results of numerical calculation for nonlinear steady state convection, developing from the respective instability, are reported along with those for a slightly wavy membrane. Besides these results, we report those of time dependent calculations for periodic and chaotic oscillations, resulting from instability of the respective steady state flows, and also the results of recent experiments with modified membranes. These latter rule in favor of electro-osmotic versus bulk electroconvective origin of overlimiting conductance through ion exchange membranes.

PACS number(s): 66.10.−x, 82.45.+z, 47.20.−k

I. INTRODUCTION

Concentration polarization (CP) is the electrochemical nickname for a complex of effects related to the formation of concentration gradients in electrolyte solution adjacent to a permselective (charge selective) solid/liquid interface upon the passage of an electric current. This is, in particular, a basic element of charge transfer across ion exchange electrodialysis membranes. The specific aspect of CP we address here concerns the stationary voltage/current (V-C) curves of highly permselective cation exchange membranes which typically are of general form depicted in Fig. 1. The following three regions are distinguishable in such a curve. The low current ohmic region I is followed by a plateau (region II, the ''limiting current'') of a much lower slope. Inflection of the V-C curve at the plateau is followed by region III, in which the slope of the V-C curve is somewhat lower than in region I. Inflection of the V-C curve (transition to region III) is accompanied by the appearance of a low-frequency excess electric noise [1–3]. Noise amplitude increases with the distance above the threshold and may reach up to a few percent of the appropriate mean value.

Steady state passage of an electric current higher than the limiting one through an ion exchange membrane is commonly referred to as overlimiting conductance. The mechanisms of it and of the accompanying excess electric noise remained unclear for a long time. It has been shown conclusively that no such mechanisms as loss of membrane permselectivity at high voltage or the appearance of additional charge carriers (''water splitting'') are responsible for these phenomena at cation-exchange membranes [4–8].[1]

Eventually, a fair amount of indications have been accumulated, suggesting that the overlimiting behavior of the ion exchange membranes has to do with some kind of convective mixing that develops spontaneously in the depleted diffusion layer at the advanced stage of concentration polarization [4,9–11]. This has been finally confirmed by a direct experimental observation: if the depleted diffusion layer is immobilized by a gel, a plateau is reached at saturation, and the excess electric noise disappears [12].

It was suggested that gravitational convection, brought about by the density gradients due to concentration polarization, may destroy the unstirred layer [9,10]. It should however be remembered that gravitational instability of a laminar sublayer at a smooth solid/liquid interface in a well mixed bulk flow may occur only upon the fulfillment of quite general hydrodynamic conditions. Thus, whatever the nature of the bulk flow, laminar or turbulent, natural or forced, gravitational instability will destroy an already existing horizontal diffusion layer with a positive upward density gradient only if the respective Rayleigh number is above a critical value that is larger than 1000. For an aqueous, 200-μm thick or less diffusion layer of a 0.01 or 0.1 molar NaCl solution the Rayleigh number is 11.6 and 116, respectively, that is at least an order of magnitude below the instability threshold. Electroconvection, in particular, the one driven by nonequilibrium electro-osmotic slip at the solution/membrane interface, was suggested as an alternative mechanism drawing together the overlimiting phenomena at cation exchange membranes [13–18].

Two types of electroconvection in strong electrolytes may be distinguished: bulk electroconvection, due to the action of the electric field upon the residual space charge of a locally quasielectroneutral electrolyte with nonuniform concentration, and convection induced by electro-osmotic slip of either equilibrium (first) or nonequilibrium (second) kind, discussed in this paper. Both types of electroconvection may set on either in a thresholdless manner due to inhomogeneity of membrane surface (mechanical, such as roughness or conductive) or with a threshold, through instability of quiescent electric conduction. Electroconvection of both types has

*Email address: robinst@bgumail.bgu.ac.il
†Email address: boris@bgumail.bgu.ac.il

[1]This is also true for anion exchange membranes, although there the aforementioned overlimiting pattern is obscured by the fact that most anion exchange membranes intensely ''split water'' in the course of concentration polarization due to a particular catalytic surface reaction [6–8].

 ©2000 The American Physical Society

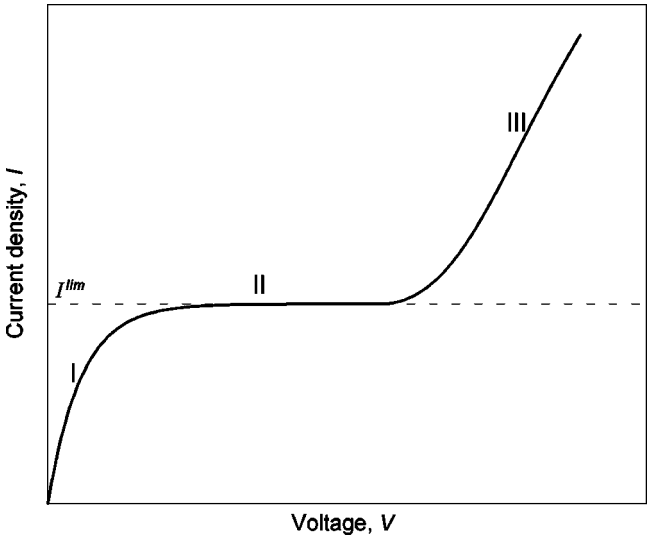

FIG. 1. Sketch of a typical dimensionless voltage-current curve of a cation-exchange membrane.

been invoked, besides the membrane context [15,16] as a factor effecting the dendritic pattern formation in electrodeposition [19–21] and layering of colloid crystals on electrode surfaces [22,23]. Study of bulk electroconvective instability has been initiated by Grigin [24]. In his paper Grigin used the lowest order Galerkin approximation to study the critical perturbation mode for unrealistic boundary conditions [24,25]. The main focus of this pioneering work was the possibility of bulk electroconvective instability. Grigin's papers were followed by an independent study by Bruinsma and Alexander in which they investigated the bulk electroconvective instability in a very narrow polarization cell of finite thickness for galvanostatic conditions [26] which likely amounted, in terms of concentration polarization in a flat layer, to consideration of some very particular perturbation mode. A systematic numerical study of linear bulk electroconvective instability in an electric layer flanked by cation-selective surfaces has been carried out for galvanostatic conditions in Refs. [16,27].

So far we know of no efficient numerical solution for nonlinear bulk electroconvection, and, thus, we do not know whether the aforementioned bulk electroconvective instability may actually develop into a major mixing mechanism on a macroscopic (diffusion layer) scale. Based on heuristic energy balance arguments, Bruinsma and Alexander claim in Ref. [26] that it may not.

In our recent experiments aimed at distinguishing between the bulk electroconvective and electro-osmotic mechanisms in overlimiting conductance we cast micron to submicron thick layers of aqueous conductive solid (cross-linked polyvinylalcohol) on the surface of a cation-exchange membrane [28]. Usage of this thus modified membrane in concentration polarization tests in a thin polarization cell [12,13] showed that immobilization of electrolyte in the vicinity of the depleted solution/membrane interface resulted in elimination of overlimiting conductance. Considering the negligible thickness of the immobilized layer compared to that of the diffusion layer (200 μm in the polarization cell employed), this indicates in favor of the electro-osmotic mechanism of overlimiting conductance versus the bulk electroconvective one.

In our previous publications [17,18] we developed theory of nonequilibrium electro-osmotic slip at a permselective membrane (electro-osmosis of the second kind [29]). It has been shown that this slip yields instability of the quiescent concentration polarization at a homogeneous membrane. Electroconvection, developing from this instability , results in destruction of the diffusion layer, causing overlimiting conduction. Not far above the instability threshold, steady state electroconvective vortices start oscillating in a periodic manner. Upon further moving away from that threshold, these oscillations soon become chaotic, resulting in low frequency excess electric noise, typical of the overlimiting conductance. Besides the derivation of the electro-osmotic slip condition and the linear stability analysis, Refs. [17,18] contained a brief account of preliminary results pertaining to nonlinear convection at either homogeneous or inhomogeneous membrane. In this paper we present a systematic account of the respective results for a homogeneous membrane.

Thus, in largely introductive Sec. II, besides the formulation of the basic model problem, we outline the derivation of the slip condition and recapitulate the main results of the linear stability analysis. In addition to the respective results in Ref. [18] we present here the wave number dependence of the linear growth rate. In Sec. III we present the results pertaining to the stationary nonlinear vortex size selection. In Sec. IV we describe the loss of stability by those steady electroconvective vortices, resulting in the appearance of their periodic, and later, chaotic oscillations and the spectral properties of their related excess electric noise. Finally, in Sec. V, as a possible application, we discuss precipitation of the onset of overlimiting conductance by a slight periodic distortion of the flat membrane surface on the length scale of diffusion layer thickness.

II. ELECTRO-OSMOTIC SLIP OF THE SECOND KIND AND INSTABILITY OF QUIESCENT CONCENTRATION POLARIZATION AT A PERMSELECTIVE MEMBRANE

The prototypical two-dimensional model problem for concentration polarization in a diffusion layer of a univalent electrolyte adjacent to a permselective membrane under the passage of a normal electric current in the dimensionless form reads [17,18,30] (tilded notations are used below for the dimensional variables, as opposed to their untilded dimensionless counterparts):

Equations for the diffusion layer $\{-\infty<x<\infty,\ 0<y<1\}$:

$$c_t^+ + \mathrm{Pe}(\underline{v}\nabla)c^+ = D\nabla(\nabla c^+ + c^+\nabla\varphi), \tag{1}$$

$$c_t^- + \mathrm{Pe}(\underline{v}\nabla)c^- = \nabla(\nabla c^- - c^-\nabla\varphi), \tag{2}$$

$$\varepsilon^2\Delta\varphi = c^- - c^+, \tag{3}$$

$$\frac{1}{\mathrm{Sc}}\underline{v}_t = -\nabla p + \Delta\varphi\nabla\varphi + \Delta\underline{v}, \tag{4}$$

$$\nabla\underline{v} = 0. \tag{5}$$

The Nernst-Planck equations (1) and (2) describe convective electrodiffusion of cations and anions, respectively. Equation (3) is the Poisson equation for the electric potential, where $c^+ - c^-$ on the right-hand side is the space charge due to a local imbalance of ionic concentrations. The Stokes equation (4) is obtained from the full momentum equation by omitting the nonlinear inertia terms. Finally, Eq. (5) is the continuity equation for an incompressible solution. Spatial variables in Eqs. (1)–(5) have been nondimensionalized with the diffusion layer thickness L, whereas,

$$t = \frac{\tilde{t} D_-}{L^2}, \tag{6}$$

$$c^+ = \frac{\tilde{c}^+}{c^0}, \tag{7}$$

$$c^- = \frac{\tilde{c}^-}{c^0}, \tag{8}$$

$$\varphi = \frac{F\tilde{\varphi}}{RT}, \tag{9}$$

are, respectively, the dimensionless time, concentrations of cations and anions, and the electric potential, with D_- the anion diffusivity, c_0 the specified (bulk) concentration at the outer edge of the diffusion layer, F the Faraday constant, R the universal gas constant, and T the absolute temperature; $\underline{v}$ and p in Eqs. (4) and (5) are the dimensionless velocity vector and pressure, defined as

$$\underline{v} = \frac{\tilde{\underline{v}}}{v_0} = u\underline{i} + w\underline{j}, \tag{10}$$

$$p = \frac{\tilde{p}}{p_0}, \tag{11}$$

with the typical velocity v_0 and pressure p_0 determined from the force balance in the dimensional version of the momentum equation (4) as

$$v_0 = \frac{d(RT/F)^2}{4\pi\eta L}, \tag{12}$$

$$p_0 = \frac{\eta v_0}{L}, \tag{13}$$

where d is the dielectric constant of the solution (in the Gauss system) and η is the dynamic viscosity of the fluid. Below we list and discuss the dimensionless parameters in the system, Eqs. (1)–(5).

(1) The dimensionless Debye length ε is defined as

$$\varepsilon = \frac{(dRT)^{1/2}}{2F(\pi c_0)^{1/2} L}, \tag{14}$$

ε^2 lies in the range $0.2\times10^{-12} < \varepsilon^2 < 2\times10^{-5}$, for a realistic macroscopic system with $10^{-4} < L(\mathrm{cm}) < 10^{-1}$, $10^{-4} < c_0(\mathrm{mol}) < 1$.

(2) The Peclet number Pe is defined as

$$\mathrm{Pe} = \left(\frac{v_0 L}{D_-}\right) \tag{15}$$

or, using Eq. (12),

$$\mathrm{Pe} = \left(\frac{RT}{F}\right)^2 \frac{d}{4\pi\eta D_-}. \tag{16}$$

As indicated previously [30], Pe does not depend on c_0, L, and for a typical aqueous low molecular electrolyte is of order unity (more precisely, $\mathrm{Pe} \simeq 0.5$).

(3) Sc is the Schmidt number defined as

$$\mathrm{Sc} = \frac{\nu}{D_-}. \tag{17}$$

Here ν is the kinematic viscosity of the fluid.

(4) Finally, the relative cationic diffusivity D is defined as

$$D = \frac{D_+}{D_-}, \tag{18}$$

where D_+ and D_- are the dimensional cationic and anionic diffusivities, respectively.

Boundary conditions:

$y = 0$ (cation permselective membrane surface)

$$(c_y^- - c^- \varphi_y)|_{y=0} = 0. \tag{19}$$

Condition (19) states impermeability for anions of an ideally permselective cation exchange membrane

$$c^+|_{y=0} = p_1. \tag{20}$$

This condition, prescribing interface concentration equal to that of the fixed charges inside the membrane (p_1), is asymptotically valid for $p_1 \gg 1$ and amounts to disregarding the co-ion invasion of an ideally permselective membrane and the presence of an $O(\varepsilon/\sqrt{p_1})$ thick boundary layer on the membrane side of the interface

$$\varphi|_{y=0} = -V. \tag{21}$$

This condition, valid for the so called potentiostatic operation, specifies at value V (voltage) the potential drop across the diffusion layer; V is the control parameter in our treatment

$$\underline{v}|_{y=0} = 0. \tag{22}$$

This is the common nonslip condition.

$y = 1$ (outer edge of the diffusion layer):

$$c^+|_{y=1} = 1, \tag{23}$$

$$c^-|_{y=1} = 1. \tag{24}$$

Conditions (23) and (24) specify the unity dimensionless ''bulk'' concentration in accord with the aforementioned scaling

$$\varphi|_{y=1} = 0. \tag{25}$$

The normalization condition (25), together with Eq. (21), specifies an arbitrary constant in the definition of electrostatic potential

$$u_y|_{y=1}=0, \tag{26}$$

$$w|_{y=1}=0. \tag{27}$$

Conditions (26) and (27) prescribe a vanishing normal velocity and viscous shear stress at the outer ''free'' edge of the diffusion layer.

When time dependent situations are addressed, the boundary value problem, Eqs. (1)–(5) and (19)–(27), is supplemented by a suitable set of initial conditions.

The boundary value problem, Eqs. (1)–(5) and (19)–(27), possesses a one-dimensional quiescent conduction solution with $\underline{v}=0$, and c^+, c^-, and φ satisfying the boundary value problem

$$(c_y^+ + c^+\varphi_y)_y=0, \tag{28}$$

$$(c_y^- - c^-\varphi_y)_y=0, \tag{29}$$

$$\varepsilon^2\varphi_{yy}=c^- - c^+, \tag{30}$$

$$(c_y^- - c^-\varphi_y)|_{y=0}=0, \tag{31}$$

$$c^+|_{y=1}=1, \tag{32}$$

$$c^-|_{y=1}=1, \tag{33}$$

$$c^+|_{y=0}=p_1, \tag{34}$$

$$\varphi|_{y=1}=0, \tag{35}$$

$$\varphi|_{y=0}=-V, \tag{36}$$

and

$$p(y)=\tfrac{1}{2}\varphi_y^2+p_c, \tag{37}$$

where p_c is an arbitrary integration constant.

For quasiequilibrium conditions the solution of the boundary value problem, Eqs. (28)–(36), splits into the ''outer'' locally electroneutral solution, valid in the ''bulk'' of the segment $0<y<1$, and the ''inner'' or electric double layer solution, valid in the ε vicinity of the interface at $y=0$ [17,18,30]. The inner and outer solutions are connected through the standard procedures of matched asymptotic expansions. The outer leading order solution is that to the quasielectroneutral boundary value problem

$$(\overline{c}_y+\overline{c}\overline{\varphi}_y)_y=0, \quad 0<y<1, \tag{38}$$

$$(\overline{c}_y-\overline{c}\overline{\varphi}_y)_y=0, \tag{39}$$

$$\overline{c}(1)=1, \tag{40}$$

$$\overline{\varphi}(1)=0, \tag{41}$$

$$(\overline{c}_y-\overline{c\varphi_y})|_{y=0}=0, \tag{42}$$

$$(\ln\overline{c}+\overline{\varphi})|_{y=0}=\ln p_1-V. \tag{43}$$

Here $\overline{c}\overset{\text{def}}{=}c^+=c^-$, and Eq. (43) expresses the continuity of the electrochemical potential of cations (capable of penetrating the interface at $y=0$) across the discontinuities of the electric potential and ionic concentration, modeling the electric double layer in the outer problem. The outer (quiescent concentration polarization) solution is obtained by a straightforward integration of the boundary value problem, Eqs. (38)–(43), in the form

$$\overline{c}(y)=\frac{I}{2}y+1-\frac{I}{2}, \tag{44}$$

$$\overline{\varphi}(y)=\ln\left(\frac{I}{2}y+1-\frac{I}{2}\right), \tag{45}$$

where

$$I\overset{\text{def}}{=}(\overline{c}_y+\overline{c}\overline{\varphi}_y) \tag{46}$$

is the electric current density in the system. Expression (45) yields the current-voltage relation

$$I=2(1-e^{(V-\ln p_1)}. \tag{47}$$

From Eq. (47), when $V\to\infty$, $I\to I^{\lim}=2$ and, simultaneously, by Eq. (44), $\overline{c}(0)\to 0$. This is the key feature in the classical picture of concentration polarization—saturation of the current density toward the limiting value, resulting from the vanishing interface electrolyte concentration at the cathode. In fact, currents much greater than the limiting one are readily passed through virtually ideally permselective cation-exchange membranes (overlimiting conductance mentioned in Sec. I). Search for a mechanism for this and the related occurrence of the excess electric noise, provided the main motivation for the study of electroconvection in strong electrolytes in general [15–18,31–34] and the present study, in particular.

In order to investigate the stability of the quiescent concentration polarization solution, Eqs. (44)–(47), one has to allow for lateral motions. In this case too the problem splits into that for locally quasielectroneutral bulk and the boundary (electric double) layer at the membrane/solution interface. Equations describing the ionic transfer and fluid flow in the bulk read [15]

$$\overline{c}_t+\mathrm{Pe}(\overline{\underline{v}}\nabla)\overline{c}=D\nabla(\nabla\overline{c}+\overline{c}\nabla\overline{\varphi}), \tag{48}$$

$$\overline{c}_t+\mathrm{Pe}(\overline{\underline{v}}\nabla)\overline{c}=\nabla(\nabla\overline{c}-\overline{c}\nabla\overline{\varphi}), \tag{49}$$

$$\frac{1}{\mathrm{Sc}}\overline{\underline{v}}_t=-\nabla\overline{p}+\Delta\overline{\varphi}\nabla\overline{\varphi}+\Delta\overline{\underline{v}}, \tag{50}$$

$$\nabla\overline{\underline{v}}=0, \tag{51}$$

whereas the boundary layer analysis provides, in addition to boundary conditions, Eqs. (42) and (43), an expression for

electro-osmotic slip, that is the tangential fluid velocity at the outer edge of the electric double layer.

For electro-osmotic slip at a conductive permselective interface two fundamentally different regimes should be distinguished in accordance with the magnitude of the electric current through the interface.

The first (quasiequilibrium electro-osmosis, or electro-osmosis of the first kind, following terminology of Dukhin [29]) pertains to currents below the limiting value. For such currents the diffuse part of the electric double layer preserves its common quasiequilibrium structure essentially identical with that for zero current. Theory of quasiequilibrium electro-osmosis at a permselective interface was developed by Dukhin [35]. An essential part of this theory is accounting for polarization of the electric double layer by the applied tangential electric field resulting, in particular, in major lateral pressure drops in the double layer due the lateral variation of the Maxwell stresses. This results, for the tangential velocity u in the double layer, in the equation of the form

$$-\tfrac{1}{2}[(\varphi_z)^2]_x+\varphi_x\varphi_{zz}+u_{zz}=0, \tag{52}$$

where $z=y/\varepsilon$ is the boundary layer coordinate. For a quaisiequilibrium boundary layer, potential $\varphi(x,z)$ in Eq. (52) is substituted from the solution of the Poisson-Boltzmann equation

$$\varphi_{zz}=\overline{c}(x,0)(e^{\varphi-\overline{\varphi}(x,0)}-e^{-\varphi+\overline{\varphi}(x,0)}) \tag{53}$$

of the form

$$\varphi(x,z)=\overline{\varphi}(x,0)+2\ln\frac{e^{\varsigma/2}+1+(e^{\varsigma/2}-1)e^{-z\sqrt{2\overline{c}(x,0)}}}{e^{\varsigma/2}+1-(e^{\varsigma/2}-1)e^{-z\sqrt{2\overline{c}(x,0)}}}. \tag{54}$$

Here $\overline{c}(x,0)$, $\overline{\varphi}(x,0)$ are, respectively, the electrolyte concentration and the electric potential at the outer edge of the electric double layer and

$$\varsigma(x)=\varphi(x,0)-\overline{\varphi}(x,0) \tag{55}$$

is the dimensionless ς potential.

Integration of Eq. (52) with Eq. (54) yields for the electro-osmotic slip velocity, instead of the common Helmholtz-Smoluchowski formula

$$u_s=\varsigma\overline{\varphi}_x \tag{56}$$

valid for an impermeable interface, the expression

$$u_s=\varsigma\left(\overline{\varphi}_x+\frac{\overline{c}_x}{\overline{c}}\right)-4\frac{\overline{c}_x}{\overline{c}}\ln\frac{1+e^{\varsigma/2}}{2}. \tag{57}$$

The peculiarity of Eq. (57) is that, for an ideally permselective cation-exchange membrane maintained at a constant potential ($\ln\overline{c}+\overline{\varphi}=$const, that is, $\overline{c}_x/\overline{c}=-\overline{\varphi}_x$) and $\varsigma\to-\infty$, Eq. (57) yields

$$u_s=-(4\ln 2)\overline{\varphi}_x. \tag{58}$$

That is, the factor at $-\varphi_x$ (electro-osmotic factor) tends to a maximal upper value upon the increase of ς (negative). This stands in contrast with the respective prediction of the Helmholtz-Smoluchowski formula, Eq. (56), and is a direct consequence of polarization of the electric double layer at a permselective interface.

Hydrodynamic stability of the quiescent concentration polarization with a limiting quasi-equilibrium electro-osmotic slip, Eq. (58), was studied in Ref. [36]. It was concluded that electro-osmotic instability of the first kind, although possible in principle near the limiting current, was unfeasible for any realistic low molecular aqueous electrolyte. This conclusion followed from the fact that an electro-osmotic factor at least one order of magnitude higher than the limiting value $4\ln 2$ is required for this type of instability to occur. This conclusion is valid as long as the system, in particular the electric double layer, remains at quasiequilibrium. Namely, this ceases being the case when the current approaches the limiting value. We already saw that in this case $\overline{c}\to 0$ and $\overline{\varphi}\to-\infty$, which makes Eq. (53) formally unsuitable for calculation of φ in the double electric layer and, thus, through Eq. (52), for calculation of electro-osmotic velocity u_s. This reflects a fundamental structural change which occurs in the system as it moves away from quasiequilibrium upon $I\to I^{\lim}$.

Generally, quasiequilibrium is typified by the division of the system into a locally quasielectroneutral bulk and a quasiequilibrium boundary layer (diffuse double electric) layer. This picture breaks down upon $I\to I^{\lim}$ as reflected, in particular, in the inconsistency of the local electroneutrality approximation, which appears in the basic concentration polarization solution Eqs. (44)–(47) in this limit. Indeed, according to Eq. (45)

$$\varphi_{yy}(0)=\frac{I^2}{4}\frac{1}{\left(1-\dfrac{I}{2}\right)^2}\to\infty, \quad \text{when } I\to I^{\lim}=2.$$

This implies that for any finite ε, however small, setting the left-hand side of the Poisson equation (3) equal to zero becomes inconsistent. This was the motivation behind the study of the space charge of the nonequilibrium electric double layer, which develops in the course of concentration polarization when the interface concentration approaches zero and, accordingly, the local Debye length tends to infinity [37]. This study essentially consisted of a numerical solution of the one-dimensional model problem, Eqs. (28)–(37).

In Figs. 2(a) and 2(b) we present schematically the ionic concentrations and space charge density profiles obtained in Ref. [37] (and in a number of studies that followed, [30,38,39]) for a sequence of applied voltage V.

The respective results may be summarized as follows. For $0<V=O(1)$ $(I<I^{\lim})$, local electroneutrality holds in the entire system except for the boundary layer of the order of thickness ε at the left edge of the region. In the respective electroneutral region a linear ionic concentration profile holds in accordance with Eq. (44). The maximal slope of the concentration profile in these conditions is 1 (which corresponds to $I=I^{\lim}=2$). This picture remains essentially valid up to $V=O(|\ln\varepsilon|)$ $(I\leqslant I^{\lim})$. For $O(|\ln\varepsilon|)<V<O(\varepsilon^{-1})$ $(I$

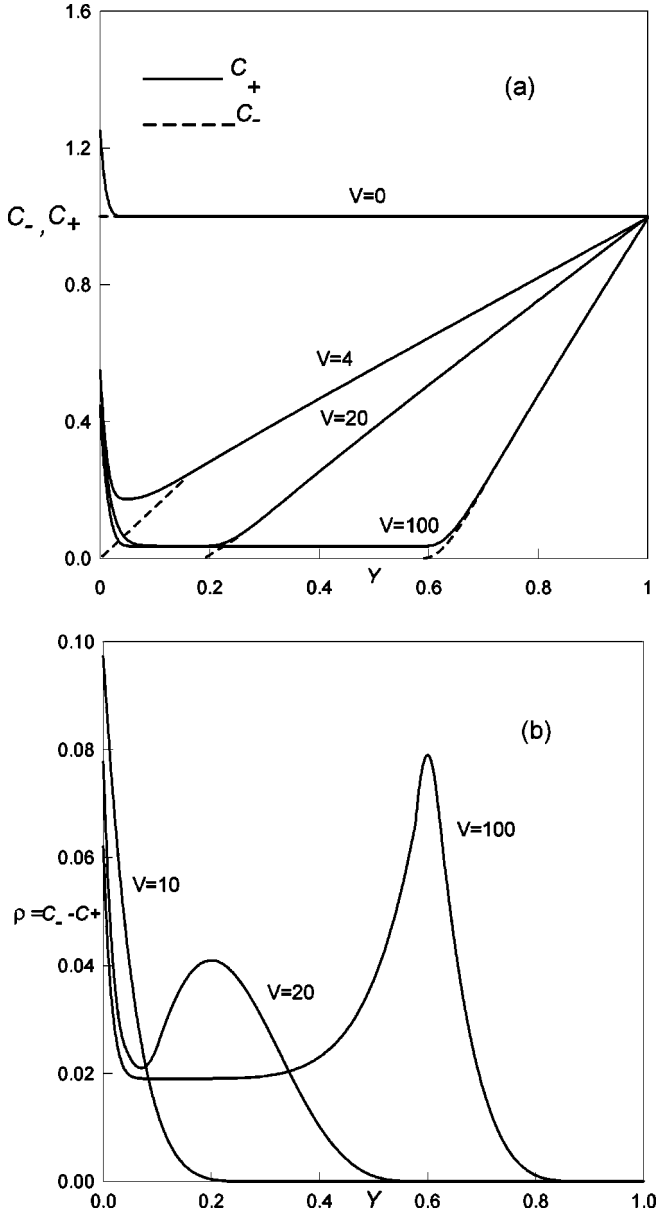

FIG. 2. Sketch of the dimensionless ionic concentrations (a) and space charge density (b) profiles in the diffusion layer and nonequilibrium electric double layer ($\varepsilon = 10^{-2}$).

$\approx I^{\lim}$), the following three regions may be distinguished (from right to left).The quasielectroneutral ''bulk'' region has a linear concentration profile with the slope of approximately 1. This region borders on the left with the extended diffuse space charge region of a width between $O(\varepsilon^{2/3})$ and $O(1)$, followed by the quasiequilibrium, $O(\varepsilon)$ thick, boundary layer at the left edge. Upon a further increase of voltage up to $O(\varepsilon^{-1})$ the extended space charge region reaches a finite size $O(1)$ and so does the current increment over the limiting value $[0 < I - I^{\lim} = O(1)]$.

The main, and perhaps the only importance of this observation of development in the course of concentration polarization of a nonequilibrium electric double layer with the extended space charge region, lays in its contribution to the discovery of the so called electrokinetic phenomena of the second kind by Dukhin and his colleagues [14,29,40] (see also references in [29]).

Accurate analysis of nonequilibrium electro-osmotic slip at a flat permselective membrane with an applied voltage V $[V > O(|\ln \varepsilon|)]$ was carried out in Ref. [18], resulting in the expression

$$u_s = -\frac{1}{8} V^2 \left. \frac{\dfrac{\partial^2 c}{\partial x \partial y}}{\dfrac{\partial c}{\partial y}} \right|_{y=0} . \tag{59}$$

Derivation of Eq. (59) employed the asymptotic theory of the nonequilibrium double electric layer, previously developed by Listovnichy [41], and amounted to carrying out an analysis similar to that outlined above for quasiequilibrium electro-osmosis. An account for polarization proved to be the more necessary here, since a large potential drop between the membrane surface and the bulk was concerned: that is, namely those conditions for which saturation of the electro-osmotic factor occurred for a quasiequilibrium electro-osmotic slip. For obtaining a better physical insight into expression (59), it is worth noting that $c_y|_{y=1}$ is one half the local current density through the membrane, which is the main local characteristic controlling the thickness of the nonequilibrium double electric layer and, thus, the electric potential in it. Noticeable also is the complete absence of the electric field from Eq. (59). As shown below this greatly simplifies the computations of the resulting bulk flow.

Summarizing, the relevant problem for time dependent ion transfer in the quasielectroneutral diffusion layer $\{-\infty < x < \infty, 0 < y < 1\}$ at a permselective solid/liquid interface reads, omitting overbars,

$$\left(1 + \frac{1}{D}\right)(c_t + \mathrm{Pe}\, \underline{v} \nabla c) = 2 \Delta c, \tag{60}$$

$$-v = u \underline{i} + w \underline{j}, \tag{61}$$

$$\frac{1}{\mathrm{Sc}} \cdot \underline{v}_t = -\nabla p + \Delta \underline{v}, \tag{62}$$

$$\nabla \underline{v} = 0, \tag{63}$$

$y = 1$:

$$c|_{y=1} = 1, \tag{64}$$

$$u_y|_{y=1} = 0, \tag{65}$$

$$w|_{y=1} = 0, \tag{66}$$

$y = 0$:

$$c|_{y=0} = 0, \tag{67}$$

$$w|_{y=0} = 0, \tag{68}$$

$$u \left|_{y=0} = -\frac{1}{8} V^2 \left. \frac{\dfrac{\partial^2 c}{\partial x \partial y}}{\dfrac{\partial c}{\partial y}} \right|_{y=0} . \tag{69}$$

We reiterate that boundary conditions Eqs. (67)–(69), are specific for electro-osmosis of the second kind, whereas Eqs. (64)–(66) are the standard boundary conditions at the outer edge of the diffusion layer, corresponding to a specified (unity) ''bulk'' concentration, vanishing normal velocity and no shear. The Coulombic term $\Delta\varphi\nabla\varphi$ [compare with Eq. (4)] has been omitted from Eq. (62) due to its $O(\ln^2 V/V^2)$ smallness for electro-osmosis of the second kind [18].

With $c(x,y)$ and $\underline{v}$ determined from Eqs. (60)–(69), $\varphi(x,y)$ is found *a posteriori* from the equation of continuity of the electric current

$$\nabla(c\nabla\varphi)=0 \tag{70}$$

with boundary conditions

$$\varphi(x,1)=0, \tag{71}$$

$$c\varphi_y(x,0)=c_y(x,0), \tag{72}$$

at $y=0,1$. [Once more, condition (72) stands for impermeability of the ideally permselective cation exchange membrane for anions, whereas the normalization condition (71) specifies the arbitrary constant in the definition of the electric potential.]

The boundary value problem, Eqs. (60)–(69), possesses a trivial ''limiting'' quiescent concentration polarization solution [see Eq. (44) with $I=I^{\lim}$]

$$c_0(y)=y, \tag{73}$$

$$\underline{v}_0=u_0\underline{i}+w_0\underline{j}=0. \tag{74}$$

Below we outline the linear stability analysis of this solution (see Refs. [17,18] for details). The respective linearized problem for the perturbations $c_1(x,y,t)$ and $\underline{v}_1=u_1\underline{i}+w_1\underline{j}$ reads

$$c_{1t}+\mathrm{Pe}\,w_1=\frac{2D}{D+1}\Delta c_1, \tag{75}$$

$$\frac{1}{\mathrm{Sc}}\Delta w_{1t}=\Delta^2 w_1, \tag{76}$$

$$w_1|_{y=0}=0, \tag{77}$$

$$w_{1y}|_{y=0}=\tfrac{1}{8}V^2 c_{1yxx}|_{y=0}, \tag{78}$$

$$w_{1y}|_{y=1}=0, \tag{79}$$

$$w_{1yy}|_{y=1}=0. \tag{80}$$

Equations (75)–(80) yield a spectral problem in the form

$$\frac{D+1}{2D}\lambda\xi+bw=\xi''-k^2\xi, \quad 0<y<1, \tag{81}$$

$$w^{(4)}-\left(2k^2+\frac{\lambda}{\mathrm{Sc}}\right)w''+\left(k^4+\frac{\lambda}{\mathrm{Sc}}\right)w=0, \tag{82}$$

$$\xi(0)=0, \tag{83}$$

$$\xi(1)=0, \tag{84}$$

$$w|_{y=0,1}=0, \tag{85}$$

$$w''|_{y=1}=0, \tag{86}$$

$$w'|_{y=0}=-ak^2\xi'(0). \tag{87}$$

Here $a\overset{\mathrm{def}}{=}\frac{1}{8}V^2$, $b\overset{\mathrm{def}}{=}[\mathrm{Pe}(D+1)/2D]$; ξ and w are the Fourier transforms

$$\xi(y)=\int_{-\infty}^{\infty}e^{ikx}\overline{c}_1(x,y)dx, \tag{88}$$

$$w(y)=\int_{-\infty}^{\infty}e^{ikx}\overline{w}_1(x,y)dx \tag{89}$$

of the spatial factors $\overline{c}_1$, $\overline{w}_1$ in the $c_1(x,y,t)$, $w_1(x,y,t)$ representation

$$c_1(x,y,t)=\overline{c}_1(x,y)e^{\lambda t}, \tag{90}$$

$$w_1(x,y,t)=\overline{w}_1(x,y)e^{\lambda t}, \tag{91}$$

where k is the wave number and λ is the spectral parameter. Recall that λ with a positive real part implies instability of the quiescent limiting concentration polarization solution, Eqs. (73) and (74).

Solution of boundary value problem, Eqs. (81)–(87), yields for λ the algebraic equation

$$-\frac{\lambda}{\mathrm{Pe}\,C\sinh k}=\frac{\lambda_1\coth\lambda_1}{\mathrm{Sc}-1}+k\coth k-\frac{\mathrm{Sc}\,\lambda^*\coth\lambda^*}{\mathrm{Sc}-1}, \tag{92}$$

where

$$\lambda^*\overset{\mathrm{def}}{=}\sqrt{k^2+\lambda/\mathrm{Sc}}, \quad \lambda_1\overset{\mathrm{def}}{=}\sqrt{\lambda\frac{D+1}{2D}+k^2}$$

and

$$C=-\frac{k^2a\sinh\lambda^*}{k\cosh k\sinh\lambda^*-\lambda^*\cosh\lambda^*\sinh k}. \tag{93}$$

For a and b in the relevant range ($\mathrm{Pe}\sim 1$, $0.1<D<10$, $0<V^2<10^4$), all roots of Eq. (92) are real. Substitution of $\lambda=0$ into Eq. (92) yields the marginal stability curve in the form

$$\frac{1}{8}V^2\frac{\mathrm{Pe}(D+1)}{2D}=4\frac{\sinh k\cosh k-k}{\sinh k\cosh k+k-2k^2\coth k}\overset{\mathrm{def}}{=}f(k), \tag{94}$$

($\frac{1}{8}V^2[\mathrm{Pe}(D+1)/2D]>f(k)$ corresponds to instability). We point out the monotonic decrease of $f(k)$ with increasing k towards the ''critical'' value 4, and, accordingly, the monotonic decrease of the threshold value of V towards the limit

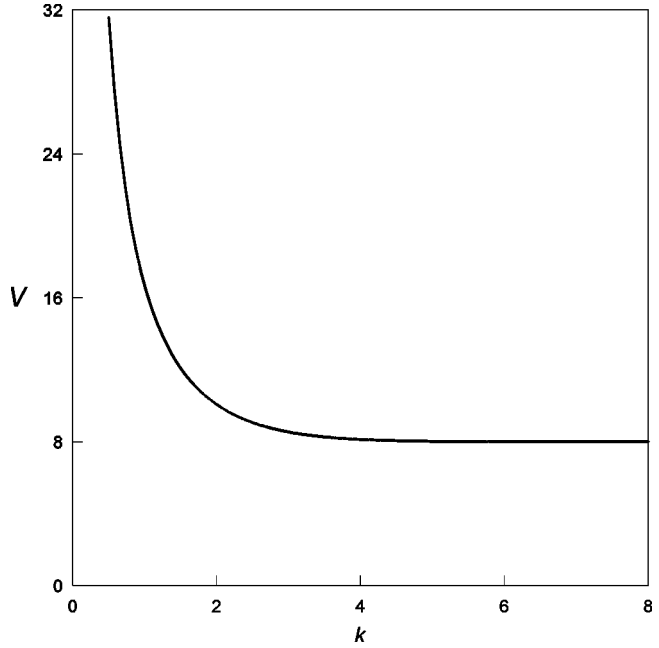

FIG. 3. Marginal stability curve for nonequilibrium electro-osmotic instability (V: dimensionless voltage, k: dimensionless wave member).

$\underline{V}=8\sqrt{D/[(D+1)\mathrm{Pe}]}$. In Fig. 3 we present the marginal stability curve as defined by Eq. (94) in the V/k plane for $\mathrm{Pe}=0.5$ and $D=1$. For linear growth rate λ Eq. (92) yields for large k

$$\lambda=\frac{(b\ \mathrm{Sc})^{1/3}}{V^{2/3}}k^{5/3}+O(k^{4/3}). \tag{95}$$

The fact that according to linear stability analysis the perturbation mode with infinitesimal wavelength is most unstable suggests the need for a nonlinear wave number selection principle. Some information in this respect is provided by the nonlinear convection computations described in Sec. III. As for a possible physical interpretation of this instability let us note that, taking into account Eqs. (46) and (72), the slip condition, Eq. (59), may be rewritten as

$$u_s=-\frac{1}{8}V^2\frac{I_\tau}{I}, \tag{96}$$

where I is the local transversal current density and subscript τ denotes differentiation in the lateral direction. For a ''seed'' circulational fluctuation at the wall, the current density drops in the direction of the circulation velocity which results, according to the minus sign in Eq. (96), in a positive feedback. For V below a certain threshold, diffusional damping dominates.

III. NONLINEAR STEADY STATE VORTEX SIZE SELECTION

In this section we present some results of a numerical solution of the full nonlinear system, Eqs. (60)–(69). We

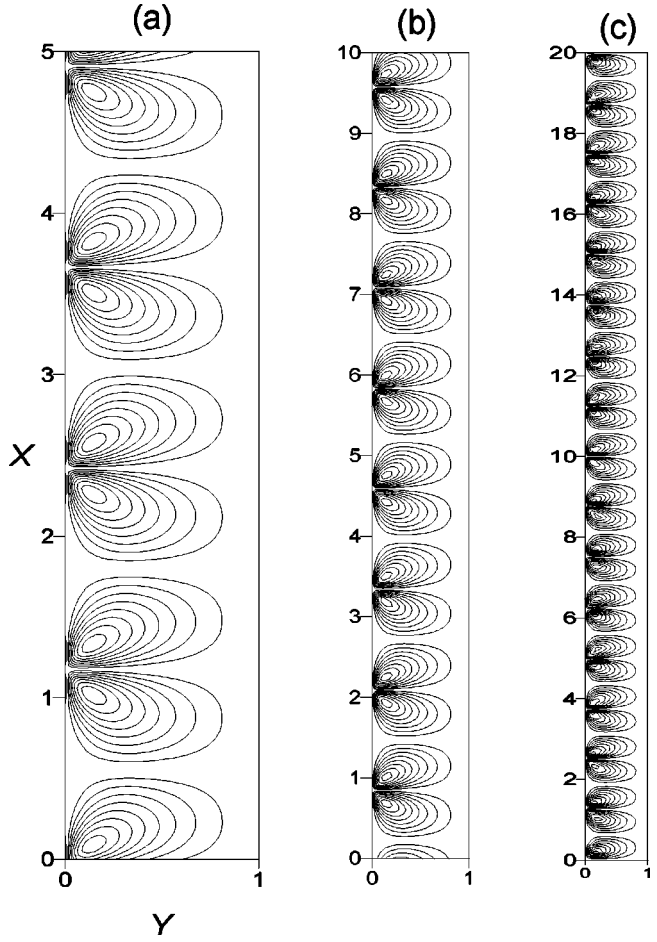

FIG. 4. Steady-state streamlines for boxes of different size (dimensionless): $H=5$ (a), $H=10$ (b), $H=20$ (c).

point out that the flow induced by electro-osmosis of the second kind is the only type of nonlinear electroconvection we have been able to investigate numerically so far.

The system [Eqs. (60)–(69)] was solved by finite differences in the domain $0<x<H$, $0<y<1$ with periodic boundary conditions at $x=0,H$ for various H and V. Thus, in Figs. 4(a)–4(c) we present the calculated families of steady state flow streamlines for $V=\underline{V}+1$ and $H=5$, 10, and 20, respectively. The qualitative image emerging from the calculations for different H may be summarized as follows. Vortices form in pairs; their size depends on H; a maximal size of H exists for a given number of vortex pairs per box; upon the increase of H above this size, an additional vortex pair appears; the maximal vortex size, corresponding to the maximal box size, roughly matches the size of vortices that emerge for an infinite layer ($H\to\infty$); this size, that is the half width of the periodicity cell formed in an infinite layer, is of order of the diffusion layer width; this reflects the general nonlinear mode selection pattern in this system as illustrated in Figs. 5–11. In these figures we present the time evolution of a family of flow streamlines starting from a short-wave periodic disturbance [Figs. 5(a)–10(a)] for $V=\underline{V}+1$, $H=2$ in six sequent time moments, in parallel with the respective Fourier spectrum of the maximum of the stream function $\Phi(x,y)$ in the normal direction y

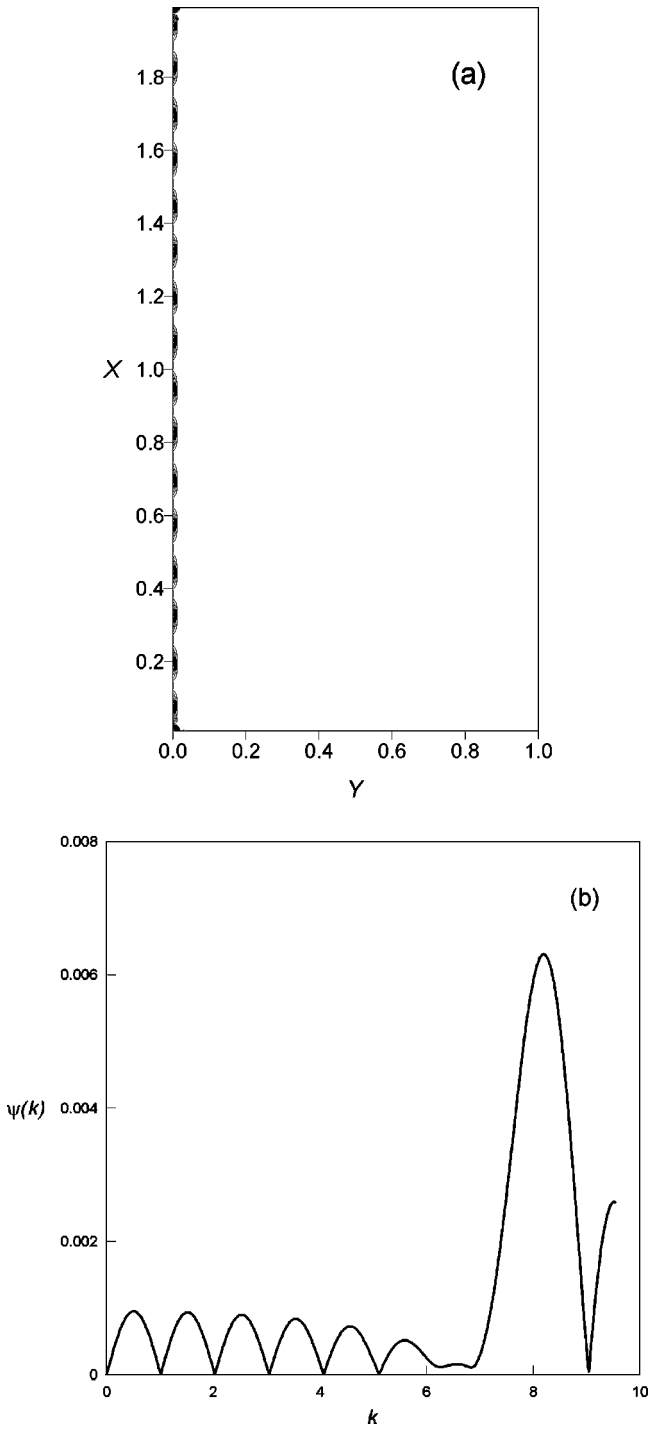

FIG. 5. Nonlinear mode selection: vortex evolution from the initial shortwave disturbance, $t=0$ (t is dimensionless time): (a) flow streamlines; (b) Fourier spectrum of the stream function's maximum.

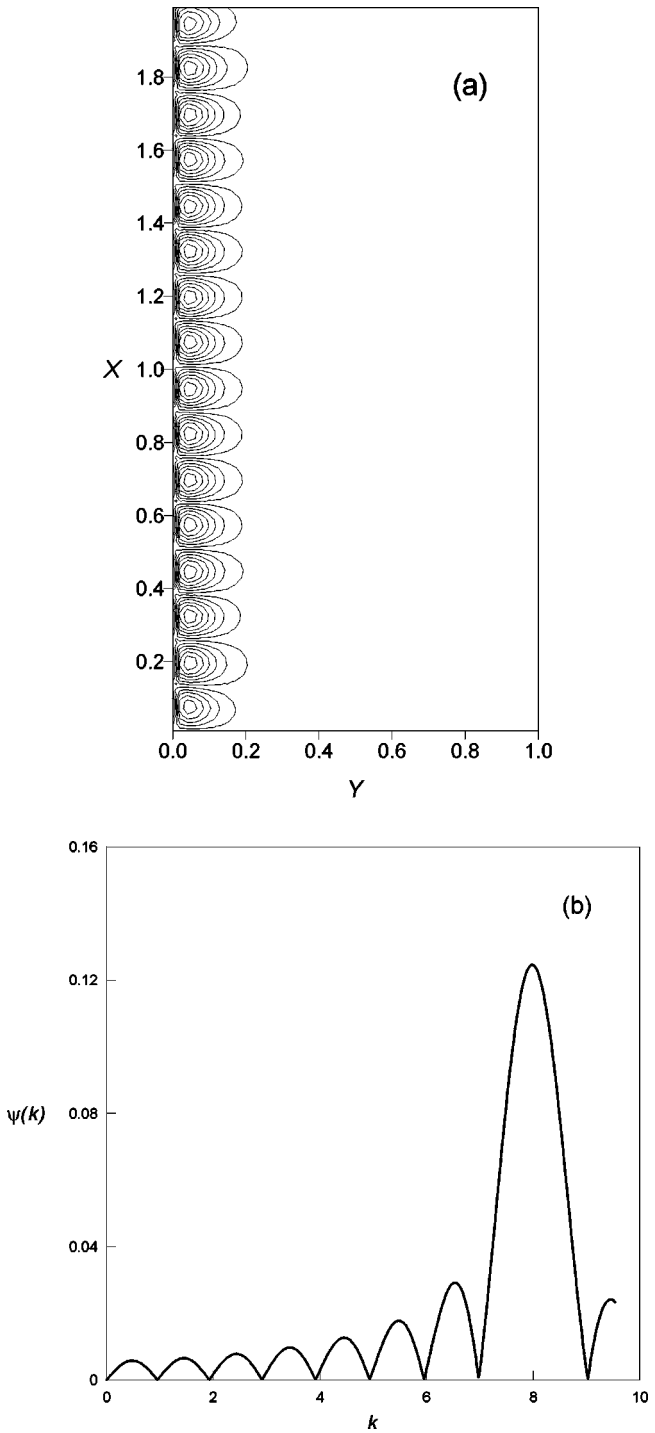

FIG. 6. Same as Fig. 5, $t=10^{-2}$.

$$\psi(k)=\left|\int_0^2 \max_{y\in[0,1]}(\Phi(x,y))e^{\pi kix}dx\right| \tag{97}$$

[Figs. 5(b)–10(b)]. The emerging picture may be summarized as follows. We begin with a very small periodic unharmonic short–wave initial disturbance [Fig. 5(a) and 5(b)] ($k=8$, eight vortex pairs) and trace its evolution subject to perturbation by a minor numerical noise. At the initial stage the short-wave modes grow faster and dominate and, thus, maximum of the Fourier amplitude appears at $k=8$ [Figs. 6(a) and 6(b)]. Eventually, these small vortices break up through fusing and form four pairs of larger vortices with a longer lifetime [see Fig. 7(a)]. Accordingly, the Fourier amplitude maximum shifts to $k=4$ with the short-wave modes remaining at a very low but finite amplitude [Fig. 7(b)]. As time goes on, these eight vortices become unstable too and start transforming into two pairs of still larger stable steady-state vortices [Figs. 8(a) and 9(a)]. In the Fourier spectrum this results in the shift of the amplitude maximum from $k=4$ to $k=2$ [Figs. 8(b) and 9(b)]. The final four stable

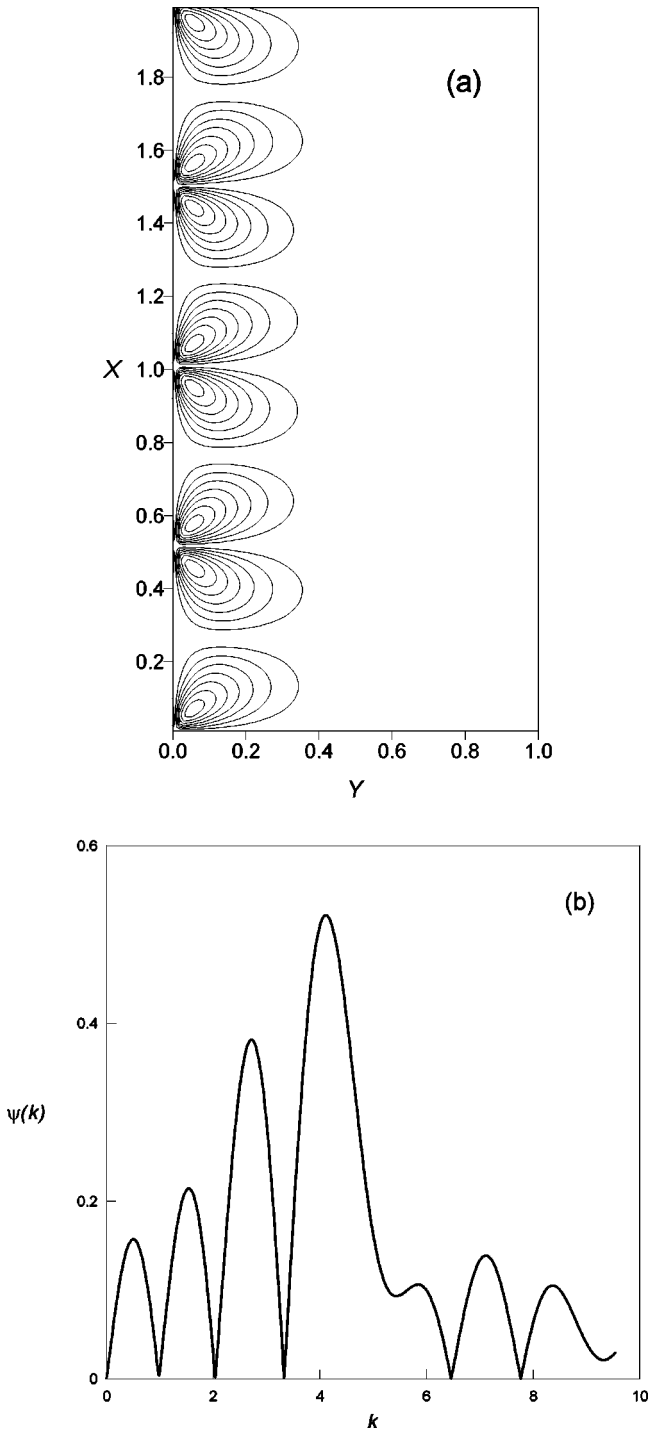

FIG. 7. Same as Fig. 5, $t=1$.

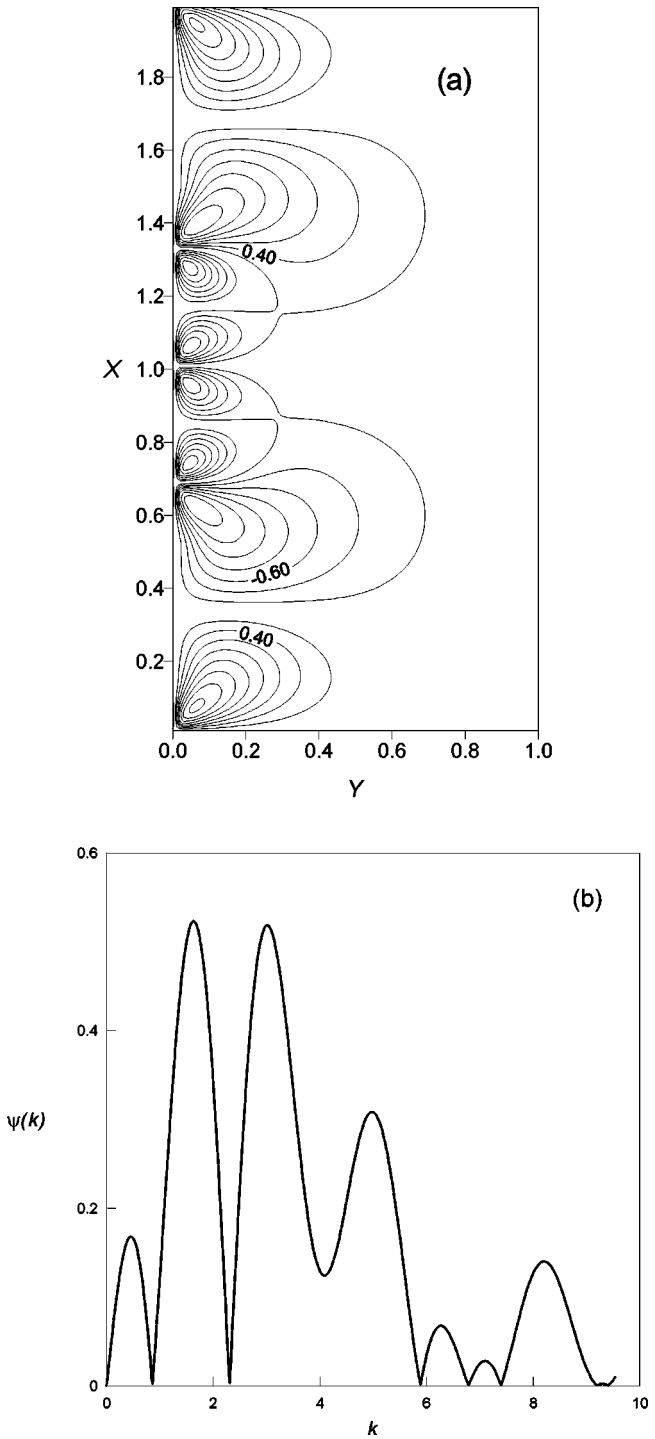

FIG. 8. Same as Fig. 5, $t=3$.

steady-state vortices and their Fourier spectrum are presented in Figs. 10(a) and 10(b).

IV. VORTEX OSCILLATIONS AND EXCESS ELECTRIC NOISE

The solution of the problem, Eqs. (60)–(69), further on from the first instability threshold $\underline{V}$ disclosed another threshold V_{cr}, depending on H ($V_{cr}\simeq\underline{V}+1.1$ for the ''infinite'' layer $H=20$) above which steady-state vortices became unstable. Namely, upon an incremental increase of voltage in the range $\underline{V}<V<V_{cr}$, transition to a new steady state occurred through a nonmonotonic, and , close to V_{cr}, decaying oscillatory readjustment of the size and shape of viscous vortices, manifesting itself in decaying oscillations of the electric current through the interface. In a narrow voltage range above the threshold the system approached the state of small amplitude periodic oscillations about a time independent average. Above this range, the attractor became chaotic. This is illustrated in Figs. 11(a)–11(c) by presenting the calculated average current density

$$\overline{I}(t)=\frac{2}{H}\int_0^H (c\varphi_y)\big|_{y=0}\,dx \tag{98}$$

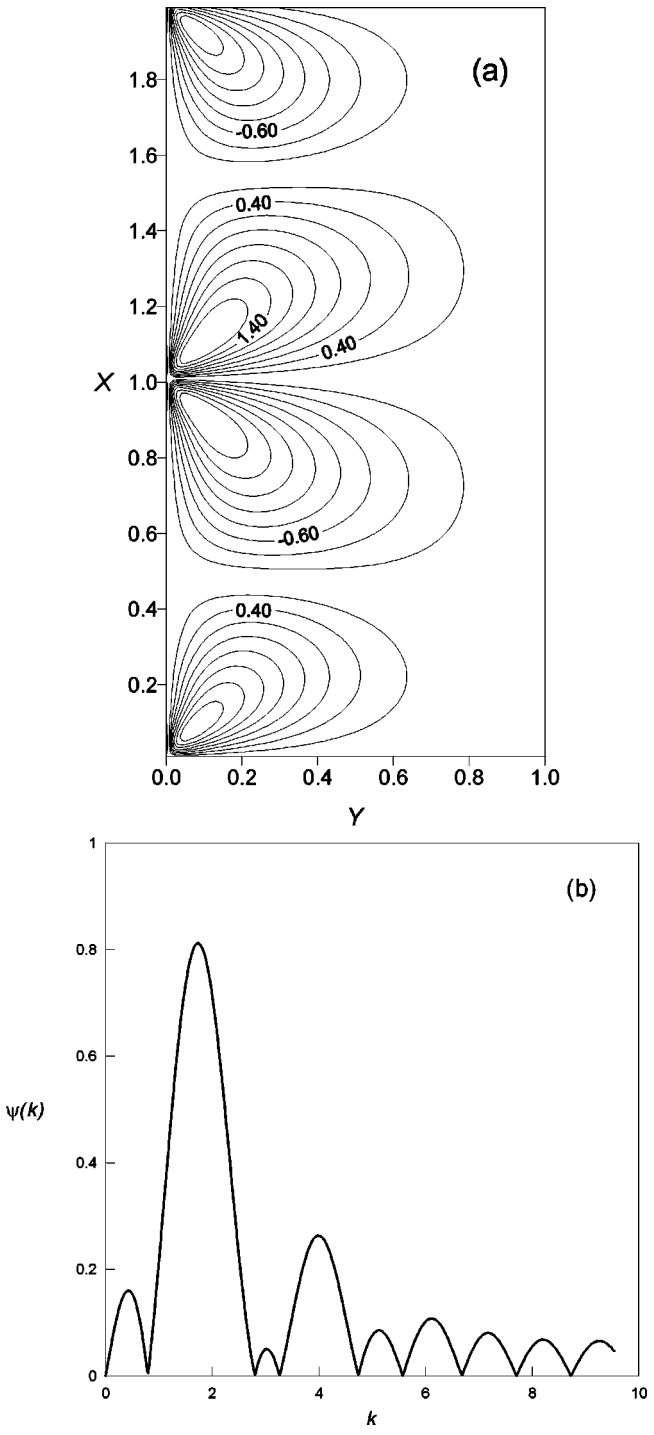

FIG. 9. Same as Fig. 5, $t=3.5$.

versus time for three sequent values of voltage ($V=\underline{V}+1$, $\underline{V}+1.1$, $\underline{V}+1.2$) for the ''infinite'' layer ($H=20$). Let us note that due to periodic boundary conditions at $x=0,H$ the average current density $\overline{I}(t)$ does not depend on y. Moreover, due to Eq. (72)

$$\overline{I}(t)=\frac{2}{H}\int_0^H c_y|_{y=0}\,dx. \tag{99}$$

For a steady state, integration of Eq. (60) over the domain $\{0<x<H,0<y<1\}$ yields, using Eq. (63), periodic boundary conditions at $x=0,H$ and Eqs. (66) and (68) at $y=0,1$

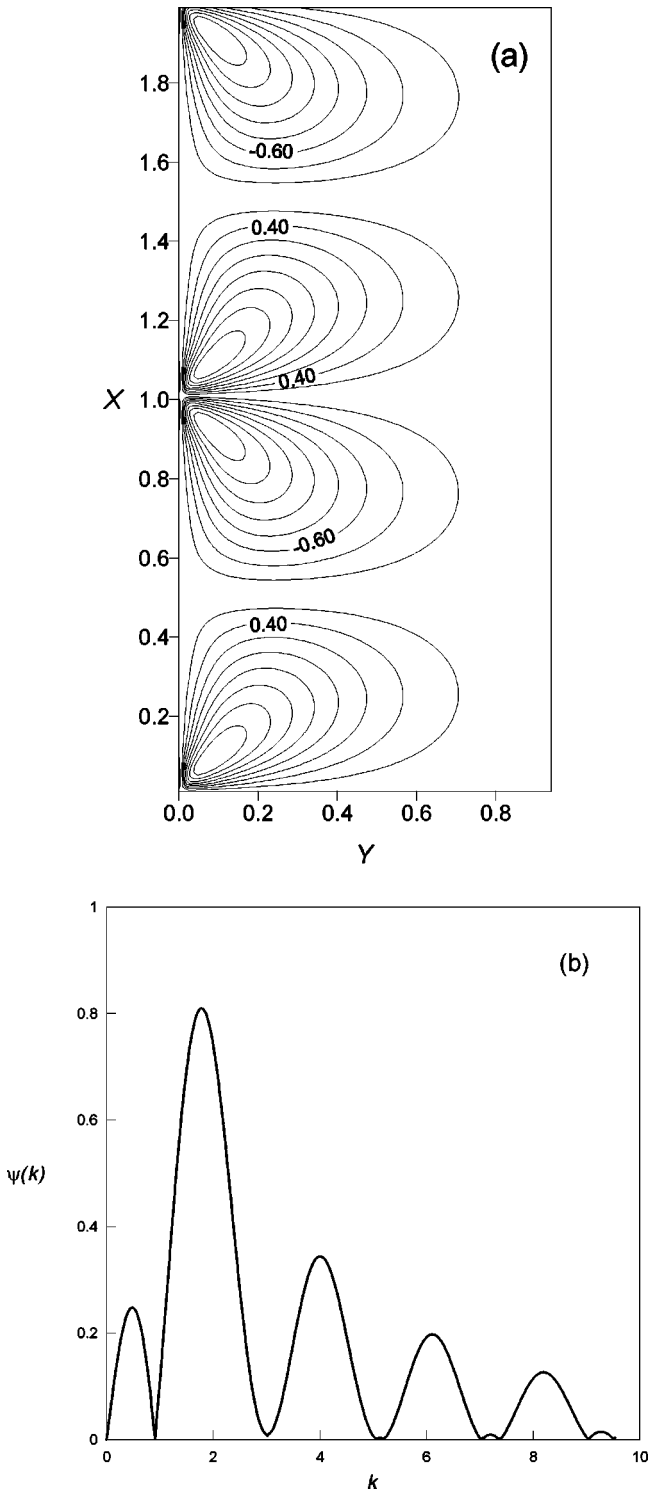

FIG. 10. Same as Fig. 5, $t=20$.

$$\overline{I}(t)=\frac{2}{H}\int_0^H c_y|_{y=1}\,dx. \tag{100}$$

Eqs. (99) and (100) provide a means for calculation of the electric current without computing the electric potential φ. For a periodic or chaotic attractor, Eq. (100) holds for the space-time averaged current density, defined as

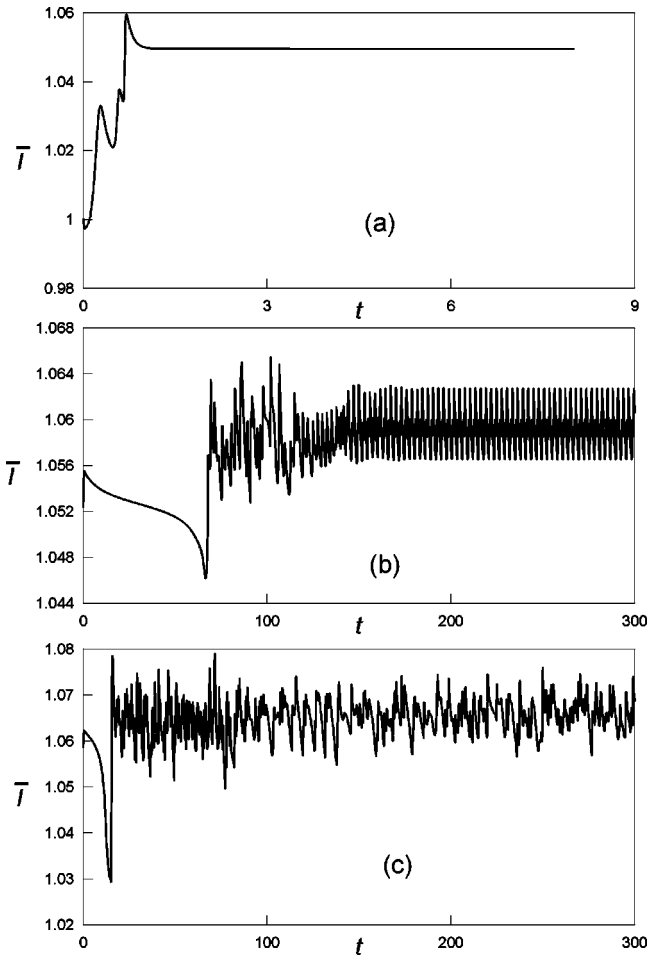

FIG. 11. Average dimensionless current density evolution towards the attractor: (a) steady state, $V=\underline{V}+1$; (b) periodic oscillations, $V=\underline{V}+1.1$, (c) chaotic oscillations, $V=\underline{V}+1.2$.

$$\overline{\overline{I}}=\lim_{T\to\infty}\frac{1}{T}\int_0^T \overline{I}(t)dt. \tag{101}$$

In Fig. 12 we present $\overline{\overline{I}}$ versus voltage curve for the ''infinite'' layer. We note the nearly linear shape of the overlimiting part of this curve.

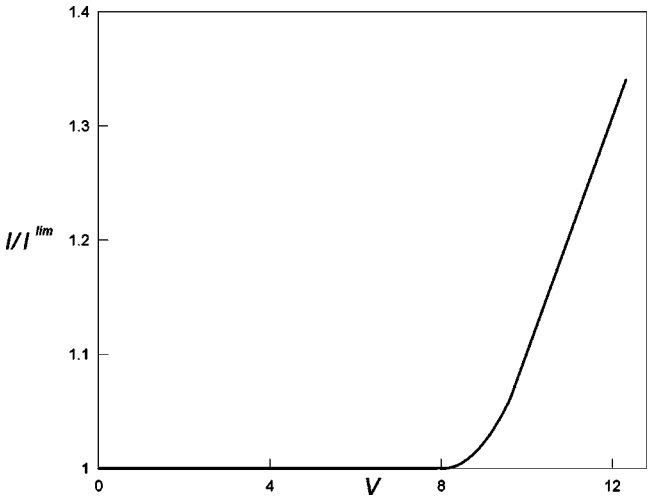

FIG. 12. Average dimensionless overlimiting current/voltage curve for an infinite flat membrane.

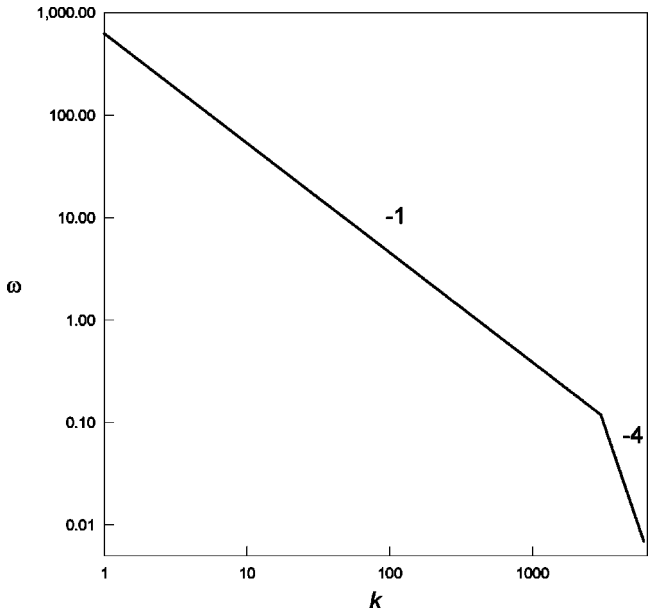

FIG. 13. Membrane noise power spectrum.

Finally, in Fig. 13 we present the calculated current noise power spectrum $\omega(k)$. The calculated noise power law exponents, $\kappa=-1$ for low frequencies and $\kappa=-4$ for high frequencies, are among those encountered in noise measurements at cation exchange membranes [1,2].

V. HASTENING THE ONSET OF OVERLIMITING CONDUCTANCE

Hastening the onset of overlimiting conductance is important for improving the efficiency of electrodialysis. In our previous publication [17] we studied the effect of nonlinear interaction of small-scale electroconvective eddies due to electric inhomogeneity of membrane surface and its possible

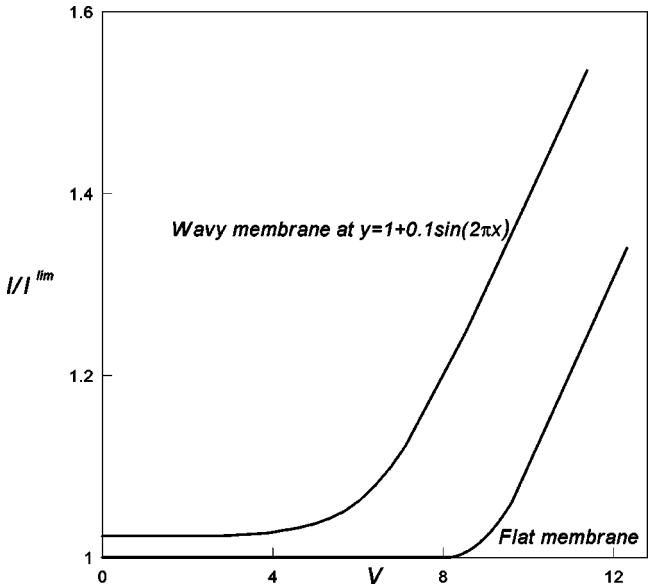

FIG. 14. Comparison of voltage-current curve for a ''wavy'' membrane with that for a flat one.

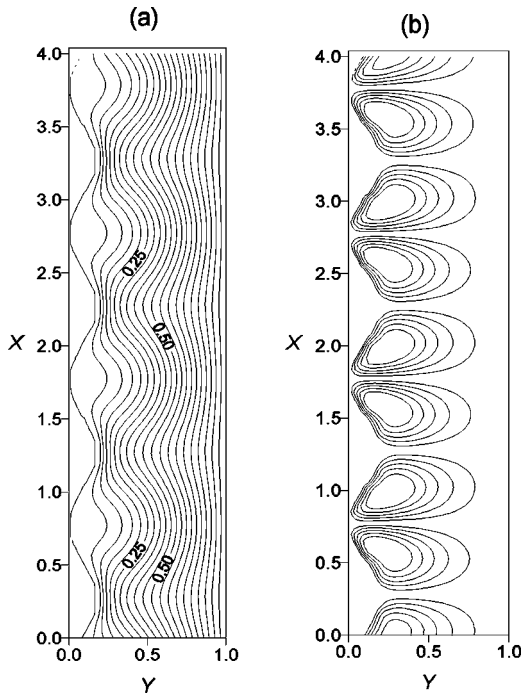

FIG. 15. Dimensionless concentration level lines (a) and streamlines (b) at a ''wavy'' membrane, $V=8.15$.

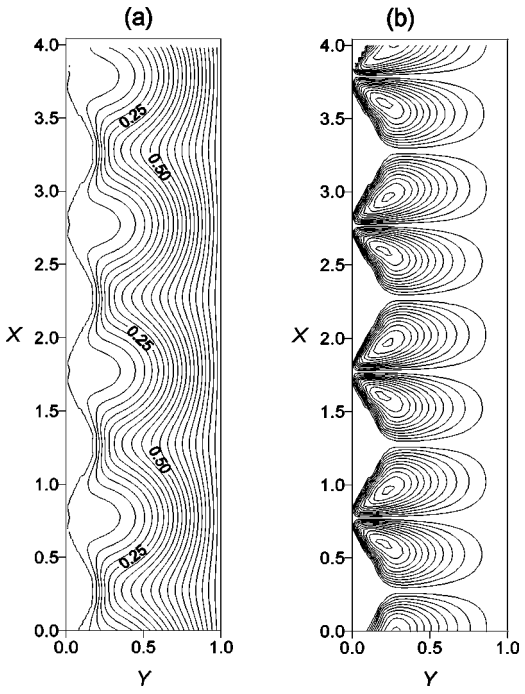

FIG. 16. Same as Fig. 15 for $V=8.65$.

role upon mixing in the diffusion layer and the onset of the overlimiting conduction. In this section, we discuss precipitation of the latter by a slight periodic distortion of the flat membrane surface on the length scale of the width of the diffusion layer. The possibility of an early onset of overlimiting conductance has already been conjectured by Dukhin and Mischuck in their pioneering paper on electroosmosis of the second kind [14].

We solved numerically the version of the full nonlinear problem, Eqs. (60)–(69), for a periodically distorted membrane surface

$$y=1+0.1\sin(2\pi x), \tag{102}$$

which required reformulation of boundary conditions, Eqs. (67)–(69) for a nonflat boundary. Nonflatness of membrane surface yields a thresholdless appearance of the vortex flow at low voltages. This convection has, however, little effect on the overall ionic transport across the diffusion layer until voltage reaches some threshold-like value upon which the overlimiting conductance sets on. Shape of the respective voltage-current curve is practically identical to that for a flat membrane, whereas a 10% distortion of the flat membrane surface results in a 30% precipitation of the onset of overlimiting conductance and a respective increase of the current compared to those for a flat membrane (see Fig. 14, slight increase of the limiting current at a ''wavy'' membrane is due to the increase of surface area compared to the flat membrane).

In Figs. 15 and 16 we illustrate the changes occurring in the diffusion layer with the increase of voltage by presenting the level lines of concentration and the stream lines for $V=8.15$ and $V=8.65$, respectively. Worth noting is the development of a low concentration zone near the concave parts of the membrane surface. For sufficiently high voltages ($V=8.65$), width of this zone reaches half of that of the diffusion layer [Fig. 16(a)].

[1] M. Yafuso and M. E. Green, J. Phys. Chem. **75**, 654 (1971).
[2] S. H. Stern and M. E. Green, J. Phys. Chem. **77**, 1567 (1973).
[3] Y. Fang, Q. Li, and M. E. Green, J. Colloid Interface Sci. **86**, 185 (1982).
[4] M. Block and J. A. Kitchener, J. Electrochem. Soc. **113**, 947 (1966).
[5] V. J. Frillete, J. Phys. Chem. **61**, 168 (1957).
[6] R. Simons, Desalination **29**, 41 (1979).
[7] R. Simons, Nature (London) **280**, 824 (1979).
[8] I. Rubinstein, A. Warshawsky, L. Schechtman, and O. Kedem, Desalination **51**, 55 (1984).
[9] S. Reich, B. Gavish, and S. Lifson, Desalination **24**, 295 (1978).
[10] S. Lifson, B. Gavish, and S. Reich, in *Physicochemical Hydrodynamics II*, edited by D. B. Spalding (Advance Publications Ltd., London, 1977).
[11] Q. Li, Y. Fang, and M. Green, J. Colloid Interface Sci. **91**, 412 (1983).
[12] F. Maletzki, H. W. Rossler, and E. Staude, J. Membr. Sci. **71**, 105 (1992).
[13] I. Rubinstein, E. Staude, and O. Kedem, Desalination **69**, 101 (1988).
[14] S. S. Dukhin and N. A. Mishchuk, Kolloidn. Zh. **51**, 659 (1989) (in Russian).
[15] I. Rubinstein, Phys. Fluids A **3**, 2301 (1991).
[16] I. Rubinstein, T. Zaltzman, and B. Zaltzman, Phys. Fluids **7**, 1467 (1995).

[17] I. Rubinstein and B. Zaltzman, in *Surface Chemistry and Electrochemistry of Membranes*, edited by T. S. Sorensen (Marcel Dekker, New York, 1998).
[18] I. Rubinstein and B. Zaltzman, Math. Mod. Meth. Appl. Sci. (to be published).
[19] V. Fleury, J.-N. Chazalviel, and M. Rosso, Phys. Rev. E **48**, 1279 (1993).
[20] V. Fleury, J. H. Kaufman, and D. B. Hibbert, Nature (London) **367**, 435 (1994).
[21] C. Livermore and P. Wong, Phys. Rev. Lett. **72**, 3847 (1994).
[22] M. Trau, D. A. Saville, and I. A. Aksay, Science **272**, 706 (1996).
[23] M. Trau, D. A. Saville, and I. A. Aksay, Langmuir **13**, 6375 (1997).
[24] A. P. Grigin, Electrokhimia **21**, 52 (1985) (in Russian).
[25] A. P. Grigin, Electrokhimia **28**, 307 (1992) (in Russian).
[26] R. Bruinsma and S. Alexander, J. Chem. Phys. **92**, 3074 (1990).
[27] J. C. Baygents and F. Baldessari, Phys. Fluids **10**, 301 (1998).
[28] Ch. Linder, Y. Oren, Y. Pretz, I. Rubinstein, and B. Zaltzman (unpublished).
[29] S. S. Dukhin, Adv. Colloid Interface Sci. **35**, 173 (1991).
[30] I. Rubinstein, *Electrodiffusion of Ions* (SIAM, Philadelphia, 1990).
[31] I. Rubinstein, B. Zaltzman, and O. Kedem, J. Membr. Sci. **125**, 17 (1997).
[32] I. Rubinstein and F. Maletzki, J. Chem. Soc., Faraday Trans. 2 **87**, 2079 (1991).
[33] T. Zaltzman, Phys. Fluids **8**, 936 (1996).
[34] T. Zaltzman, Ph.D thesis, Ben-Gurion University of the Negev, Beer-Sheva, Israel, 1996 (unpublished).
[35] S. S. Dukhin and B. V. Derjaguin, *Electrophoresis* (Nauka, Moscow, 1976) (in Russian).
[36] E. K. Zholkovskij, M. A. Vorotynsev, and E. Staude, J. Membr. Sci. **181**, 28 (1996).
[37] I. Rubinstein and L. Shtilman, J. Chem. Soc., Faraday Trans. 2 **75**, 231 (1979).
[38] V. V. Nikonenko, V. I. Zabolotsky, and N. P. Gnusin, Elektrokhimia **25**, 301 (1989) (in Russian).
[39] J. A. Manzanares, W. D. Murphy, S. Mafe, and H. Reiss, J. Phys. Chem. **97**, 8524 (1993).
[40] S. S. Dukhin, N. A. Mishchuk, and P. N. Takhistov, Kolloidn. Zh. **51**, 616 (1989) (in Russian).
[41] A. V. Listovnichy, Electrokhimia **51**, 1651 (1989) (in Russian).